AS-MAC: Utilizing the Adaptive Spreading Code Length for Wireless Sensor Networks

FEI QIN, University College London
JOHN E. MITCHELL, University College London

In many modern advanced Wireless Sensor Network (WSN) applications, the system is expected to deliver intensive traffic loads in harsh RF environment. In this paper, an MAC protocol has been proposed which will utilize the adaptive spreading code length technique to increase network performance for these applications. In this architecture, the system can automatically determine the time varying channel quality and set the optimum spreading code length to maximize the throughput while minimizing the energy usage. Due to this adaptive feature, the system is able to deliver reliable wireless service even in the harsh RF environment. The design of such a protocol is also backwards compatible to enable its employment in both traditional and advanced WSN scenarios. Finally, the proposed protocol has been implemented in a COTS WSN platform to obtain the experimental result, which demonstrates the ability of being implemented on typical resource constraints WSN devices. The experimental results have shown the efficiency advantages of the proposed MAC protocol delivering 139% higher throughput as well as having better energy performance than the standard IEEE 802.15.4 system.

Categories and Subject Descriptors: **C.2.2 [Computer-Communication Networks]**: Network Protocols

General Terms: Design, Algorithms, Performance

Additional Key Words and Phrases: Wireless sensor networks, media access control, adaptive spreading code length, channel estimation, heavy traffic load

ACM Reference Format:

Qin, F., Mitchell, J. E.. 2011. AS-MAC: Utilizing the Adaptive Spreading Code Length for Wireless Sensor Networks. ACM Trans. Sensor Network. X, X, Article XX (XX 20XX), X pages.

DOI = 10.1145/0000000.0000000 http://doi.acm.org/10.1145/0000000.0000000

1. INTRODUCTION

Wireless Sensor Networks (WSNs) have been widely promoted over the last decade, to monitor various environmental parameters, e.g. temperature, light, and humidity. Recent applications of WSNs have expanded to encompass more advanced sensing demands, for example structural health monitoring (Sukun et al., 2007), manufacturing automation monitoring (Johnstone et al., 2007), and multimedia sensor network (Rahimi et al., 2005) etc. In these advanced applications, deployed WSN have to deal with the challenge of intensive traffic load as well as the harsh RF environment. The harsh RF environment often possesses characteristics such as thermal cycling (affecting the noise floor), multi-path effects (due to stationary or

This work is jointly supported by a Dorothy Hodgkin Postgraduate Award program (BT & EPSRC sponsored) and by the Cooperating Objects Network of Excellence (CONET), funded by the European Commission under FP7 with contract numberFP7-2007-2-224053.

Author's addresses: F. Qin, J.E. Mitchell, Department of Electronic and Electrical Engineering, University College London, London, UK.. Some data of this paper has been appeared in previous publications (Fei et al.2011 and Fei et al.2012).

DOI10.1145/0000000.0000000 http://doi.acm.org/10.1145/0000000.0000000

moving metallic structures), and RF interference from machinery (i.e. brusher sparks from power generators and motors, light dimmers etc.) or other RF devices. In addition, field tests (Anritsu, 2011; Sexton et al., 2005; Tang et al., 2007) and our own investigations have revealed that these impairments are generally time-varying. These factors adversely affect the quality of the wireless communication, causing challenges, especially for WSNs with intensive traffic loads.

The adaptation of the data rate to the channel environment is inherent in the standards for IEEE802.11 (Holland et al., 2001; Kamerman & Monteban, 1997; Vutukuru et al., 2009; Zhang et al.,), Bluetooth (Chen et al., 2004) and cellular systems (Esteves et al., 2002) to maximize throughput in dynamic systems. There approaches achieve datarate adaptation by different implementation methods, the most popular of which is to adapt the modulation order, e.g. from 2-PSK to 16-QAM. To enable similar rate adaptation in WSNs, some vendors have recently released non-standard IEEE802.15.4 radio transceivers (Atmel Co.Ltd., 2009) which include spreading code length adaptation functions. In the adaptive spreading code length, the system can switch the datarate by simply changing the mapping scheme with multiple code sets in the decoding stage. In contrast, adaption of the modulation order requires several modulation and demodulation functions to be utilized, entailing the reconfiguration of the whole receiving chain rather than just the digital decoding stage. As a result, the complexity and energy consumption will increase for adaptive modulation order approaches. Considering the low cost and low energy nature of the WSNs, we suggest that adaptation of the spreading code length is a better solution. Lanzisera et al. have proposed an algorithm based on this feature to reduce the average power consumption of WSNs (Lanzisera et al.,). To the best of our knowledge, this is the only work related to the adaptive spreading code length feature in WSNs. Although this work introduced the possibility of this feature and demonstrated potential improvement through simulation, due to hardware limitations a full, practical solution with experimental validation was not presented.

This paper presents an experimentally verified MAC protocol design utilizing the adaptive spreading code length feature to achieve better performance in WSNs by increasing throughput and energy efficiency which maintaining link reliability. The motivation comes from the requirement of advanced WSNs applications, where high throughput and high reliability is needed to deal with the challenge of intensive traffic load in harsh RF environments. We suggest that the use of adaptive spreading code lengths in WSNs could be one of the most suitable candidates for these applications. Aided by the adaptive spreading code length feature, the WSN system will be able to automatically adjust the spreading code length to deliver the highest throughput for the current wireless link margin. In the case of a harsh RF environment, the system can also deliver a robust service by increasing the spreading code length when necessary (low-SNR), while decreasing the spreading length to deliver information in high data-rate mode when a high SNR is available. The WSN system deployed in an ordinary RF environment can also significantly benefit from the utilization of adaptive spreading code length, since the system will be able to deliver much higher throughput comparing with the standard IEEE 802.15.4 based WSN system. We have named the proposed MAC protocol *Adaptive Spreading – MAC*, briefly noted as *AS-MAC* for the following discussions.

However, to achieve a system performance improvement we rely on being able to determine an accurate understanding of the environment variations. As (Aguayo et al., 2004) showed, the raw SNR may not be a good indicator to predict successful delivery of data packets, due to the fading channel and device impairments. In order to improve the quality of the link estimation instead of using the SNR, some proposed methods in wireless data network (i.e. IEEE 802.11 based network) make use of learning algorithms to estimate the link quality (Vutukuru et al., 2008).

However, these learning based methods require that the sensor node must be active all the time to overhear all wireless transmissions, which is not suitable for energy constrained WSNs. Other approaches calibrate the relationship between SNR and Packet Error Rate (PER) by exchanging probe packets(Sha et al., 2009). Such operation will cause a relatively high overhead, which scales rapidly as the size of the network increases. At least one WSN deployment crashed due to the expected high volume of overhead packets (Langendoen et al., 2006). Instead, in our proposal we employ a Kalman filter based method to estimate the channel quality. This method can achieve an accurate estimation result with affordable local computation resources. This results in an algorithm this is cognitive to channel changes in a fast and energy efficient manner, which is more suitable for deployments in WSNs.

In section 2, the adaptive spreading code length technique will be briefly introduced. Based on this technique, Section 3 will discuss the detailed design of the AS-MAC, to enable the optimization of the adapted spreading code length modes from a number of different perspectives. The proposed AS-MAC has been implemented in a COTS platform to evaluate the performance. A standard IEEE802.15.4 MAC has also been implemented in the same platform as a comparison. Performance results will be provided in section 4 to demonstrate the advantage of the proposed AS-MAC. Finally, our findings will be concluded in section 5.

2. ADAPTIVE SPRAEDING CODE LENGTH IN IEEE 802.15.4 SYSTEM

In this section we outline the scheme and performance of adaptive spreading code length in the IEEE802.15.4 architecture, which is the most popular physical layer solution for wireless sensor networks. In the IEEE 802.15.4 PHY layer [2], four information bits (a symbol) are used to select one of 16 code words from a nearly orthogonal code set to be transmitted during each data symbol period. Hence, the rate adaptation will be enabled by adjusting the length of these code words. As the length of these code words increases, the data transmission rate decreases but reduced Signal to Noise Ratio (SNR) is required. Such a scheme will be an evolution of the IEEE 802.15.4 solution, compliant in its basic mode and backwards compatible. To better understand this feature, as well as, to propose a practical solution, we base our analysis and experiment on a Commercial off-the-shelf (COTS) platform, the ATMEL AT86RF231 (Atmel Co.Ltd., 2009), which supports an evolution of the adaptive spreading code length derived from the IEEE 802.15.4 standard (IEEE Std.802.15.4 Std, 2003). The standard employs 32 chips DSSS to provide a fixed 250kbps data rate at 2Mchip/s. In the AT86RF231, three additional operating modes with spreading code lengths: 4 chips, 8 chips and 16 chips along with the standard 32 chips mode are realized, which enable the experimental demonstration of the tradeoff between the data rate and the error performance.

We first designed an experiment to demonstrate the performance of different spreading code lengths, which replicates an AWGN channel by using an attenuator to model the path loss of the channel. As a result, the quality of the channel can be measured avoiding environment noise while still being fully controllable through adjustments of the attenuators. The system follows the standard IEEE 802.15.4 MAC. In this experiment, the transmitting device has been configured to work in saturation mode which means there is always a packet ready in the queue to be sent. As shown in figure 1.a, the experimental results are converted to the form of Bit Error Rate (BER) versus Receive Signal Strength (RSS) for different spreading modes. The data shown in this experiment is collected from several experiments, including changing the transmission power, the pathloss, and the environment noise. Without loss of generality, all variables have been normalized to simplify the comparison. The normalized received signal strength is defined as 'the received signal strength to achieve the same performance without any effect of additional environmental noise'.

Although the data shows a statistical variance, the overall trend for each mode is clear, and the receiver sensitivities are comparable to the sensitivity threshold provided by the datasheet of the AT86RF231 (Atmel Co.Ltd., 2009), which validates the accuracy of this result for further discussions. In figure1.b, we further show the throughput performance versus RSS, in which it is more straightforward to understand the benefit of different spreading modes. The results demonstrate several important facts which motivate and ground the discussion of this paper. First of all, by carefully choosing a spreading length mode, the system will be able to achieve an optimum mode to deliver the highest throughput. Secondly, the system is able to estimate the capacity of the wireless link accurately, which enables the optimization algorithm. Finally, since the only difference between spreading modes is the mapping choice, the power consumption is the same for all spreading lengths. To demonstrate this hypothesis, the energy consumption of the same device but configured to transmit a packet in different spreading modes by sequence, the energy consumption of this device has been captured and provided in figure 1.c with a time line format. As we expected, all four spreading modes consume the same level of energy. Therefore, the shorter of the spreading length, less power will be consumed as the time to transmit a given packet is reduced. These three facts have shown the possibility of utilizing the adaptive spreading code length to maximize the throughput while minimizing the energy consumption, and yet maintain a reliable wireless link service.

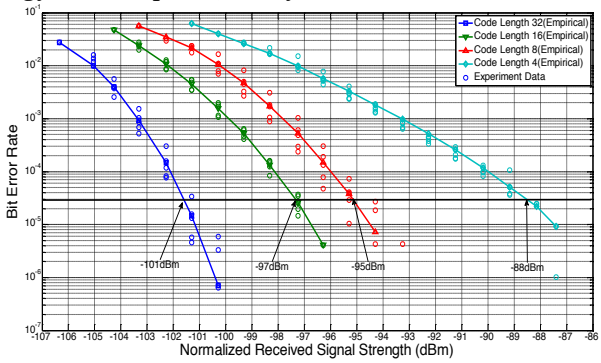

a) Error performance

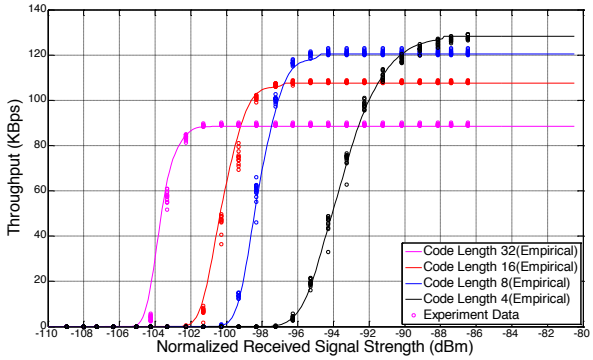

b) Throughput performance

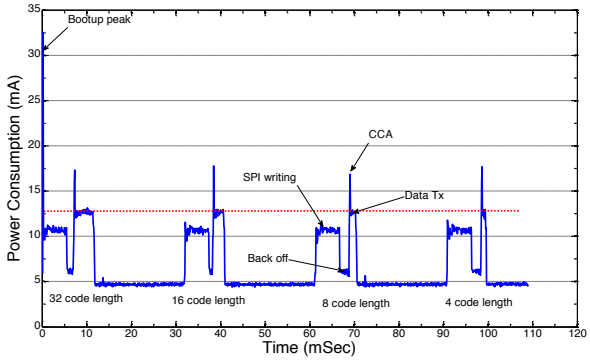

c) Power consumption performance

Fig. 1. Experimental system performances for different spreading lengths

The design of the proposed AS-MAC to utilize the adaptive spreading code length will be grounded on the findings discussed in our previous works. In (Fei Qin et al., 2011), we first experimentally identified the error performance of different spreading length modes as discussed previously.

Based on these result, an analytic model has been proposed to accurately estimate the error performance. This used a specially designed Kalman filter to estimate the channel quality of dynamic wireless channels, the results of which were used to obtain the potential channel capacity. Due to the nature of the Kalman filter, such an estimation will be able to track the condition of the time varying wireless channel much faster than other approaches, e.g. moving average. The design and implementation has been previous discussed in (Fei Qin et al., 2012).

Using this technique the receiver is able to calculate the optimum spreading code length for the current transmission link with very limited computation resources. In this paper, we will utilize the findings in our previous work as methods to design an integrated and deployable optimization based MAC protocol to apply adaptive spreading code lengths to improve the network performance and demonstrate the system throughput and energy efficiency improvements possible.

3. DESIGN OF AS-MAC PROTOCOL

The design solution will clearly be based on an effective mechanism to exchange this information between the transmitter and receiver; a feature which is not provided in the standard IEEE 802.15.4 MAC, or its variants typically used in WSNs e.g. B-MAC. Obviously, the four way hand-shake scheme currently employed by the IEEE 802.11 DCF is one of the candidates to solve this problem. However, unlike the IEEE 802.11 DCF, the maximum packet length supported by the physical layer of IEEE 802.15.4 is much smaller: only 128 Bytes. The overhead cost of RTS and CTS packets for this short packet could be too high for WSN system. This problem can be mitigated in the scenario with heavy offered traffic loads through the aggregation of packets from the application layer. Instead of directly sending out packets from the application layer, the MAC layer will buffer the packets until a block of packets are waiting for transmission and can be transmitted together in one four way hand-shake procedure.

However, this protocol must also be compatible with traditional applications with a low duty cycle as well as advanced applications with intensive data transmission tasks. It should be noted that even data intensive applications can consist of hybrid tasks, i.e. the intensive data transmissions are only triggered in a burst pattern, and the network will still need to be able to deal with single and short packets at all other time. Therefore, any proposed algorithms should consider the requirements for both kinds of transmission.

As observed previously, there will always be a large number of packets transmitted in high throughput applications and thus, we are motivated to investigate whether we could use the first packet of the queue as an RTS packet, and utilize its ACK packet as the CTS packet to exchange the optimization result generated in receiver side. If there are other packets in the queue, they could be transmitted at a faster data-rate (depend on the link quality), whereas if this is the only packet waiting to be sent the cost can be controlled, since there is no additional overhead in this procedure (the same as standard IEEE 802.15.4 MAC: one data packet and one ACK packet). In this paper we will analyze this new protocol to see if it is able to fulfill the requirements of advanced WSN applications, i.e. to provide higher throughput while maintaining energy efficiency in a low-cost design.

The details of the protocol design will be described in this section. Different aspects in the implementation will be discussed separately first and the overall architecture of the proposed AS-MAC will be presented at the end of this section.

3.1 Modifications to Carrier Sense

The design of the standard IEEE 802.15.4 MAC is very similar to the IEEE 802.11 DCF protocol but with further simplification. Such simplification is derived from the characteristics of the traditional WSNs system, i.e. low traffic load and low power oriented. For instance, the IEEE 802.11 DCF will freeze the backoff timer when the channel is busy and only decrease the backoff timer when the channel is detected to be idle. Obviously, this scheme will require the transceiver to be active to monitoring and report the wireless channel during the whole carrier sense process and will continually consume power. Therefore, in the design of the IEEE 802.15.4 MAC, this operation has been significantly simplified: as soon as a packet arrives, the MAC protocol will start the backoff timer following the same exponential manner. Unlike the IEEE 802.11 DCF scheme, the radio transceiver will be set to idle in this process to save energy and the backoff timer will continually decrease. The IEEE 802.15.4 MAC will only sense the channel after the backoff period for a fixed time slot (192 μs), and the feedback of this measurement will determine whether the channel is free or not.

As these random backoffs were employed to de-synchronize the channel competition for different devices, such a scheme works fine in extremely low offered traffic load scenarios to provide acceptable performance. In more advanced applications, although the overall offered traffic loads may still be in low level, there could be heavy offered traffic load concentrated in a short period which will cause high competition in the wireless channel, e.g. in the sample burst. In this case, such a simplified MAC scheme will greatly decrease the delivered system throughput due to low level of knowledge of the wireless channel and increased power consumption due to the higher retry and retransmission rate.

The second issue is about the carrier sense operation, which is the physical layer will enable the radio front-end for a fixed period and record the power readings of the detected signal. If the readings exceed a pre-configured threshold, a channel busy result will be reported. In a wired system, the channel can be assumed as a perfect media, therefore having only two states: occupied or free. Such a system still works fine in fully connected wireless systems (e.g. each devices in the network can communicate with each other), but will lose performance in real wireless networks due to the quantization of the wireless channel status instead of the simple on and off wired channel.

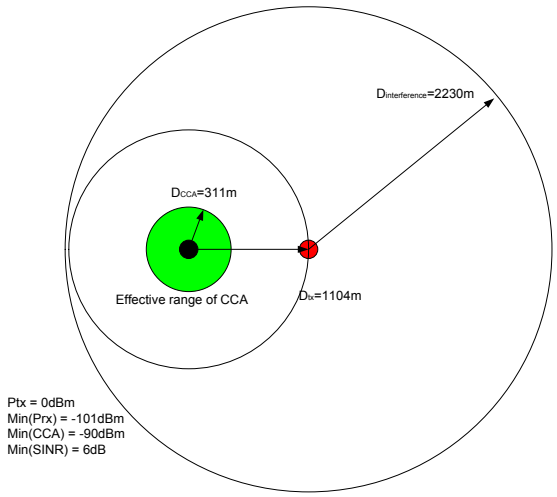

Fig. 2. Effect of carrier sense

An example has been shown in figure 2 based on the transceiver we are currently using for our experiments, but similar effects can also be expected for other IEEE802.15.4 radio transceivers. Assuming each node transmits a packet with 0dBm transmission power and that the potential receiver located inside the medium cycle in figure 2 can form a stable wireless link giving the condition that the minimum receiving sensitivity is -101dBm and the propagation model is the standard free space model (O'Rourke et al., 2007). According to the device specification (Atmel Co.Ltd., 2009), the minimum energy reading for the incoming signal is -90dBm, therefore the CCA can only be effective to in avoiding collisions with a competitor if it is located within the smallest cycle highlighted in green. Furthermore, considering that the minimum SINR requirement for a stable wireless link is 6dB, if the receiver is located in the red pot shown in the figure, any node located between the smallest circle and the biggest circle will interrupt the transmission link.

It is easy to notice that the effect of the current carrier sense operation in IEEE 802.15.4 MAC is very limited. If a higher spreading mode was employed, the Signal to Noise Ratio (SNR) requirement will be further increased which has been demonstrated in (Fei Qin & John E Mitchell, 2011). As a consequence, the wireless link will be more vulnerable to competitors in the network. Therefore, we are motivated to modify the current carrier sensing operation of the IEEE 802.15.4 MAC to improve the overall performance for an adaptive spreading code length based WSNs system. In the proposed protocol, once packets arrive from the application layer, the MAC layer will start the exponential backoff timer. However, the MAC protocol will set the transceiver to the receiving state instead of the idle state. In other words, we prefer the system to learn as much channel information as it can rather than saving small amounts of energy.

We now demonstrate that the energy consumed in this operation is relatively small compared with the whole energy consumed for a packet transmission. According to the IEEE 802.15.4 standard (IEEE Std.802.15.4 Std, 2003), the backoff period is uniformly distributed in a binary, exponentially expanding range $[0 \sim 2^{i-1}(w-1)]$, where i is the number of the retransmission and $w = 8$ is the initial backoff window size. Each backoff slot lasts 16 μs and the CCA operation after the backoff period lasts 192 μs. Then, considering that the collision probability in the traditional low traffic scenarios can be assumed to be zero, the backoff period can be approximated as $2^{i-1}(w-1)/2$. Now, we have all the parameters needed to calculate the proportion of power consumption in the backoff period within the traditional scenario, for example only *1.23%* of the energy can be saved if the packet has a payload of 100 Bytes and was transmitted with the default power of 0dBm. It is easy

to notice that keeping the transceiver idle in this operation only contributes a small proportion of the overall energy consumed. Therefore, forcing the transceiver to enter the receiving state in the backoff period will not cause significant power consumption, but this modification will assign the system more flexibility in determining the channel information. The AS-MAC will continue to read the energy detection value from the transceiver to gain information on the channel. If the channel is free, the first packet in the block will be transmitted after the backoff period. In this case, the recorded energy detection value can be assumed to be the environment noise with accumulated far away interference and will be recorded as the statistic of the environment noise.

If there are other activities in the channel (e.g. another transmission link is ongoing), two potential feedbacks can be expected. First, if such transmission was initialized during the backoff period, the preamble of that packet can be captured. Then the system will receive this packet until it finished. The signal strength and the packet information including the link parameters will be recorded to update the link status metric. Since the preamble lasts 192 μs, we also modify the duration time of each backoff slot to 192 μs instead of 16 μs to enable the carrier sensing to have enough time to capture the preamble as shown in figure 3. As a consequent, the protocol can determine the channel as busy and double the back off window. Second, if the transmission was started before the backoff period, the carrier sense can still report detection of the IEEE 802.15.4 signal, but due to the decoding implementation, we cannot force the transceiver to decode packet without recognition of the preamble. In this case, we simply assume the channel is busy and double the backoff window, and increasing the probability of capturing the preamble in the next backoff period. It is also noted that, in both cases, since different spreading modes can be employed in this protocol, the received packet may report a CRC failure due to the un-synchronized spreading mode. When a packet has been received but reported as a CRC failure, the protocol will be cycled to the next spreading mode for the next potential transmission. The scheme has also been shown in figure 3.

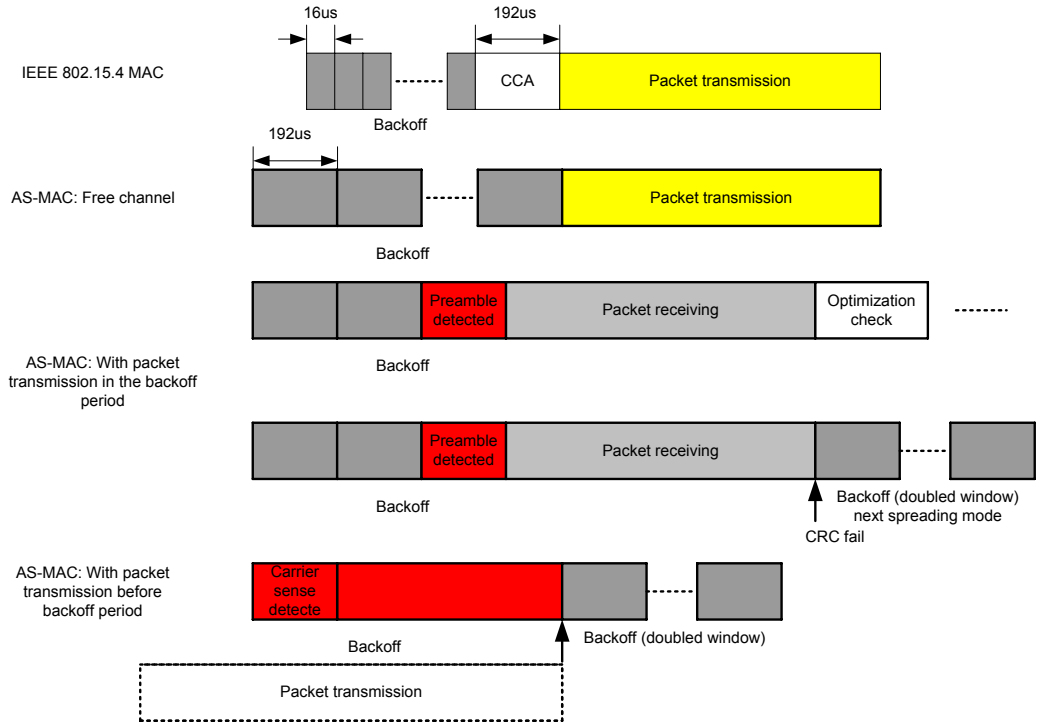

Fig. 3. Carrier sense modification in AS-MAC

We understand that it is possible to enable concurrent transmission to achieve even higher network performance. However, the current transceiver implementation will synchronize to any detected preamble even though could be a higher SNR packet arriving later. Therefore we limited this possibility in this version of protocol and defer it to our future investigation.

3.2 Packets Aggregation

Once the channel is free, the MAC layer will attempt to send the first packet in the buffer queue. In traditional WSN applications, it is most likely that the first packet is also the only packet waiting in the queue. In this case, just like the default IEEE 802.15.4 MAC, the packet will be sent out immediately. Since there is no pending packet waiting to be sent, the receiver will also process this packet in the default IEEE 802.15.4 way and send the ACK packet. The only difference is that the proposed AS-MAC will feed the signal strength of received packet to the Kalman filter to enable it tracking the channel quality trend, if any, of the current transmission link.

In advanced sensor network applications, the throughput demands from the upper layers could be much higher during the sample period. For instance, in a structural health monitoring application, the system could sample the vibration sensor with a 1 kHz sample rate, thus, every second there will be around 60 packets (with payload length = 100 Bytes) arriving from the upper layers. Another example could be multi-media based applications. Considering a system equipped with a standard 300×200 digital camera and recording static pictures every second, the raw data (i.e. BMP format) generated could be as large as 240kB. Even if the data can be locally processed with a JPEG algorithm, the data needing to be transferred via the network can still exceed 12kB (assuming 5% compression ratio), which will be converted to an offered traffic load of more than 120 packets per second. In traditional WSN applications with simple sensor inputs, the existence of aggregation congestion (i.e. the close to the sink device, the more aggregated packets from pervious hops will occur) can result in congestion of data packets in the MAC layer. These packets used to cause congestion in the traditional wireless sensor networks, but with the aid of adaptive spreading code length, the AS-MAC will be able to utilize higher bandwidth to increase the performance of WSNs in advanced applications.

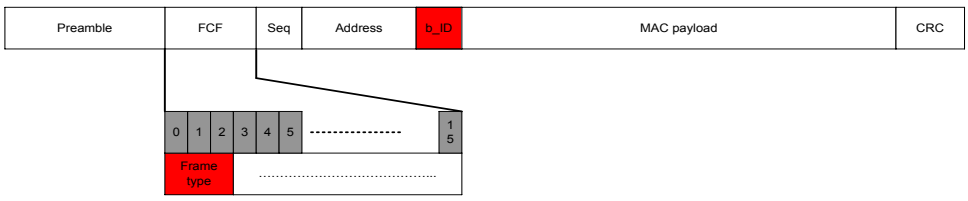

Fig. 3. Modification of the packet structure in AS-MAC

In the case where there is more than one pending packet in the queue, the AS-MAC will process them as a block, i.e. a series of packets will be transmitted in one hand shaking process. The first packet in the queue will be sent out as a probe packet. To indicate to the receiver this unique packet type, we have reused the frame type subfield in the Frame Control Field (FCF) of the IEEE 802.15.4 packet structure. Value of 0,1,2,3 have been used by the standard IEEE 802.15.4 to indicate the beacon, data, ACK, and command packets respectively. Then we define frame type 4 as the probe packet, which is the first packet in the block. After receiving the probe packet, the receiver will start the optimization algorithm based on information learnt about

the current wireless link and environment, and return the optimized result within the ACK packet. However, this special ACK packet will contain different and more important information than the standard ACK packet, thus we assign it a frame type of 5 to distinguish if from standard ACKs. After successfully decoding the first ACK, the transmitter will send the other packets in the block using the optimized configuration. These packets will be indicated with a frame type of 6. After the whole block has been transmitted, the receiver will terminate the link with a final ACK packet, which will contain the packet loss information, if any, and will be flagged with a frame type of 7. Finally, the transmitter will re-buffer the lost packets into the queue and start another cycle as long as the queue is non-empty. The packet structure has been provided in figure 4 while the basic procedure of AS-MAC has been illustrated in figure 5.

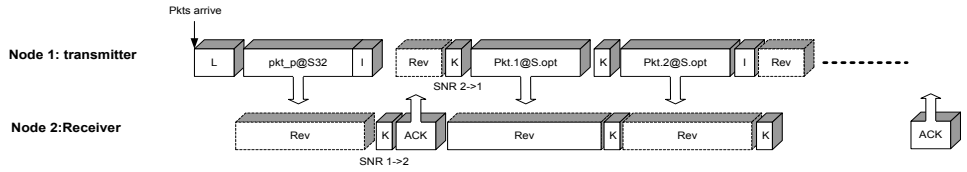

Fig. 4. Basic scheme of AS-MAC

Besides the frame type, the AS-MAC will also need to know the block-ID for each packet in the block, .e.g. to check if the packet is lost. We then have to add one more byte in the MAC header just before the payload as shown in figure 9. This block_ID will be counted from high to low, i.e., the block_ID of the probe packet will be equal to the block size, and the last packet in the block will have a block_ID of one. Therefore, the proposed AS-MAC will only increase the overhead over the standard IEEE802.15.4 MAC by one byte, which is affordable for the low-cost and resource constraint designs.

3.3 Determination of the channel quality

The first step in the optimization process is to estimate the link quality. However, published measurements (Aguayo et al., 2004) have shown that solely measuring the raw SNR during a short time scale, e.g. the duration of a packet, may not be a good predictive method to estimate the quality of wireless link, due to the fading channel and device impairments. In order to improve the quality of the link estimation, instead of the raw SNR, many recently proposed methods make use of learning algorithms to estimate the link quality. However, these learning based methods require that the sensor node must be active all the time to overhear all wireless transmissions, which is not suitable for energy constrained WSNs. Other approaches calibrate the relationship between SNR and Packet Receive Rate (PRR) by exchange probe packets (Sha et al., 2009). Such operation will cause a relatively high overhead, which is normally scalable as the size of the network increases. At least one WSN deployment crashed due to the high volume of overhead packets (Langendoen et al., 2006). We propose to make use of information redundancy among indicators provided by the IEEE 802.15.4 system to improve the estimation of the link quality. In this paper we present an empirical study showing that an improved indicator, termed Effective-SNR, can be produced by combining SNR and LQI with minimal additional overhead. The Kalman filter can be one of the best candidates in this scenario. Firstly, it can provide an accurate estimation of the current wireless link. Secondly, the estimation is not only based on the current link states but also the historic statistic. Thirdly, a Kalman filter can follow changes in link quality very rapidly, e.g. in the implementation, the system can converge with less than 10 inputs.

Furthermore, the Effective SNR processed by the Kalman filter has normalized the fading effects,, thus, it is more straightforward to calculate the best spreading code length mode with the Effective SNR measure in an AWGN channel model, rather than with raw SNR in a fading channel model. Therefore, a Kalman filter has been employed to generate the link estimation rather than the simple moving average method used in some other rate adaptive protocols.

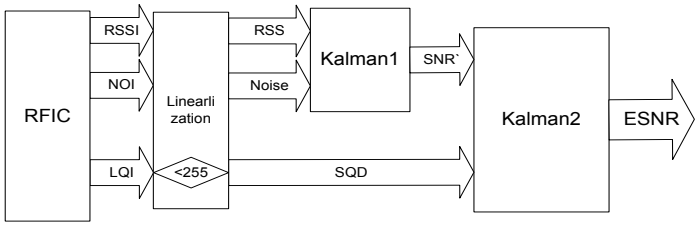

Fig. 5. Architecture of Kalman Filter

Figure 6 illustrates the structure of the proposed Bi-Kalman filter estimator. The first Kalman Filter (KF1) filters the measurement noise from the RSSI indicators while the second Kalman Filter (KF2) generates the Effective-SNR value using the information redundancy between the RSSI and LQI as input parameters and improves the Effective-SNR estimation. KF1 uses the RSSI and environment noise readings (denoted by NOI in the rest of this paper) from the RFIC as the input. Since the RSSI and NOI readings are immediately available when a packet arrives, KF1 provides a filtered SNR value once a packet is received. Because of the availability of LQI, KF2 only updates the value of Effective-SNR when the received packet's LQI is less than 255. Whereas, when the LQI is saturated (equal to 255), KF2 does not update the observed equation of KF2. In this situation the estimation is only updated by the state equations of KF2.

The first Kalman filter will be trigged by each packet received or channel assessment. The design of KF1 is to address the variation of signal strength (Received Signal Strength and environment noise N_e) by filtering the measurement noise. Although the function of KF1 is similar to the average filtering method, Kalman filtering typically gives higher accuracy with faster tracking. Considering that the packet transmission and environment noise are subjected to fading effects, RSS and N_e can be assumed to be slowly changing variables. Therefore, the system can be modeled as:

$$\begin{cases} RSS_k \approx RSS_{k-1} + w_{s,k} \\ N_{e_k} \approx N_{e_{k-1}} + w_{n,k} \end{cases} \quad (1)$$

where w_s and w_n represent the impact of fading on the signal and the environment noise, respectively. w_s and w_n are assumed independent with zero mean Gaussian distributions.

For the sake of compact notation, equation (1) can be rewritten in vector form, which gives the following state evolution equation:

$$x_k = A \cdot x_{k-1} + w_k \quad (2)$$

where $x = \begin{bmatrix} RSS \\ N_e \end{bmatrix}$ is the state variable of the dynamic system, $A = \begin{bmatrix} 1 & 0 \\ 0 & 1 \end{bmatrix}$, $w = \begin{bmatrix} w_s \\ w_n \end{bmatrix}$. It can be seen that the state variable can be observed by the RFIC directly and is subject to measurement noise, which is mainly contributed by the internal noise. Therefore, the observation equation can be written as:

$$y_k = H \cdot x_k + v_k \quad (3)$$

where $y = \begin{bmatrix} P_{rss} \\ NOI \end{bmatrix}$, $H = \begin{bmatrix} 1 & 0 \\ 0 & 1 \end{bmatrix}$, and $v_k = \begin{bmatrix} v \\ v \end{bmatrix}$. v is the measurement noise vector caused by the impairment of hardware

Once the state space model has been setup by equations (7~9), the associated Kalman filter is straightforward (Kalman, 1960).

Priori Update: $x_k^- = A \cdot x_{k-1}^-$ (4)

Priori Error covariance: $P_k^- = A \cdot P_{k-1} \cdot A^T + Q$

Kalman Gain: $K_k = (P_k^- \cdot H^T) \cdot (H \cdot P_k^- \cdot H^T + R)^{-1}$

Posteriori Update: $x_k = x_k^- + K_k \cdot (y_k - H \cdot x_k^-)$

Posteriori Error covariance: $P_k = (I - K_k \cdot H) \cdot P_k^-$

where x_k^- is the *a priori* estimation of state, x_k is the posteriori estimation of state, $P_k^- \in R^{2\times2}$ is the *a priori* estimated error covariance, $P_k \in R^{2\times2}$ is the *a posteriori* estimated error covariance. $K_k \in R^{2\times2}$ is the Kalman gain, Q is the variance of state noise, R is the variance of measurement noise. Since the initial value P does not affect the optimal value of K, a non-zero marix can be assigned to P as the initial value, and K will automatically converged to the optimal value. The appropriate values of P and Q will be determined empirically and discussed in the next section.

The second Kalman filter is trying to utilize the redundancy between SNR and LQI. It was noticed that the LQI is highly correlated with the PRR. Therefore, it is possible to map the LQI to the corresponding PRR value, which can be further converted to the SNR requirement in the AWGN channel by applying the analytic model described in (Fei Qin & John E Mitchell, 2011). Now, we will have two SNR value, the first one is detected in the real channel with possible fading influence, while the second one is the estimated value to achieve same PRR in the AWGN channel. We then term the difference between these two values as the Signal Quality Degradation (SQD). Unlike the first Kalman filter, the second Kalman filter can only be trigged if the LQI of received packet is less than 255. Once the second Kalman filter has been activated, it will use the output of the first Kalman filter as one of its measurements through a simply deduction of two states variables.

$$x_{2,k} = A_2 \cdot x_{2,k-1} + w_{2,k} \quad (5)$$

where $x_2 = \begin{bmatrix} SNR \\ SQD \end{bmatrix}$, $A_2 = \begin{bmatrix} 1 & 0 \\ 0 & 1 \end{bmatrix}$, and $w_2 = \begin{bmatrix} w_{snr} \\ w_{sqd} \end{bmatrix}$. w_{snr} and w_{sqd} represent the effect of fading on the SNR, from the view of the signal strength and signal distortion respectively, which are assumed to be independent and with zero mean Gaussian distributions.

The observation equation can be written in equation (6).

$$y_{2,k} = H_2 \cdot x_{2,k} + v_{2,k} \quad (6)$$

where $y_2 = \begin{bmatrix} SNR \\ ESNR \end{bmatrix}$, $H_2 = \begin{bmatrix} 1 & 0 \\ 1 & -1 \end{bmatrix}$, and $v_2 = \begin{bmatrix} v_{SNR} \\ v_{LQI} \end{bmatrix}$. v_{SNR} and v_{LQI} are the measurement noise caused by tolerances in the hardware design.

In common with the evolution of KF1, the second Kalman Filter can be solved by applying equation (4) to the model described in equation (5-6). Note that, the parameter matrices of KF1 (i.e., A,B,C,D, P, Q, etc.) in (4) should be replaced by the parameter matrices of KF2, respectively.

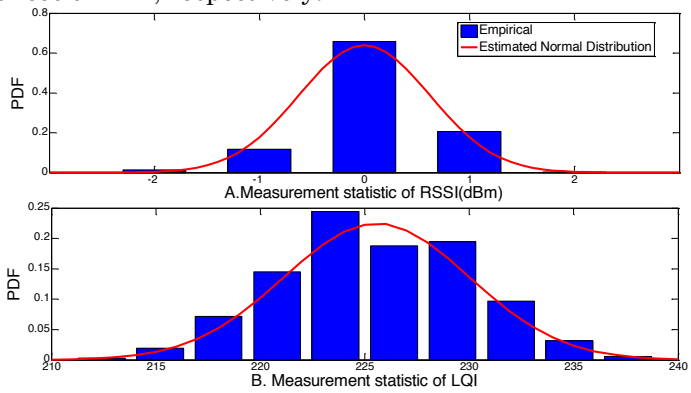

Fig. 6. Measurement noise

The variance of the measurement noise can be accurately calculated through the same experiment utilized in section 2. In such an experiment the values of transmission power and path-loss are set manually, external noise removed and fading negated. Therefore, it is reasonable to consider this as the true value of received signal strength. This can be validated with standard measurement equipment, i.e. a spectrum analyzer. We are then able to determine the measurement noise through a comparison between the RSS measured and the RSSI measurement produced. Using the statistic methods, it is straightforward to calculate the variance R as shown in figure 7.A. Due to the manufacturing and components tolerances, the devices used exhibit slightly differing performance parameters. As shown in figure 7.B, a similar method can be employed to determine the variance of the LQI detection and finally calculate the measurement variance of Effective-SNR.

From our experiment, it was seen that the dynamic range of the metric used in the Kalman filter is relatively small and bounded. Therefore, we suggest that it is unnecessary to employ floating point numbers in this implementation. Without significant loss of accuracy, the 16-bit fixed point method with a scale of 128 (i.e. a measurement of 1 will be scaled to 128, giving a resolution around 0.01 and a full-scale of [-256~256]) was employed. Nevertheless, fixed point calculations can be used for the Kalman filter implementation which result in a decrease in the computation time from 2.14ms to 0.2ms in our implementation. Considering that the normal packet delivery time could be between 5 to 10ms, such computation time can be easily accepted in WSNs. In addition, we see that the energy consumption of the calculations required are much smaller than that of transceiver operations. MCUs like the Atmega128 and the MSP430 (which are the most popular MCU in WSNs), require less than 4mA, while the receiving state of RF transceiver RF231 requires more than 15 mA. Hence, we try to trade off increased calculations against the number of probe exchanges and longer receiving periods. As the Kalman filter will only require an additional 0.2ms of processing time, the energy consumption of the proposed Kalman filter will be less than 1% of a normal packet receiving operation.

With the help of proposed Kalman filter as well as the modification of channel assessment described in section 3.1, the system will be able to learn and track the varying link quality for each of the potential receiver and monitored transmission pair. The Effective-SNR for all the neighbor devices will be stored for the optimization process.

3.4 Optimization of the optimum spreading code length

Once the receiver has detected a packet, the AS-MAC will first check the frame type field. If the frame type of the packet is equal to the probe packet type, the optimization process will be triggered. The optimization process's aim is to maximize the deliverable throughput in the current wireless link without interrupting any existing wireless link. This target can be achieved theoretically by maximizing the following function:

$$\max_{r \in R} Throughput(r) \tag{7}$$

where R is the set of the data rates for all possible spreading code length modes.

For each transmission link, given the SINR and the packet length for the current link request, equation (7) can be derived into the following equation (8), i.e. minimizing the Packet Error Rate (PER) by choosing the right spreading code length.

$$\min_{r \in R} PER(r) \tag{8}$$

Algorithm 1. Pseudo code of optimization process

```
Spreading_code_length_optimization(Effective-SNR, Packet_length)
{
 minPER = 1;
 best_r = -1
 if (converge_Kalman()!=1)
{
  return 0;
}
 for all r∈R
 {
   SER= get_SER(Effective-SNR);
   PER=(1 − SER )^(2·packet_length);
   if (PER < minPER)
    {
      minPER = PER;
     best_r = r;
    }
 }
 return best_r;
}
```

As shown in Algorithm 1, once the AS-MAC has detected a probe packet and triggered the optimization process, it will first check whether the Kalman filter has converged. If not, the optimization process will return the default spreading code length mode, i.e. 250 kbps. The optimization will only have effect when the Kalman filter has converged, i.e. it is able to provide an accurate estimation. Then the AS-MAC will use the estimated Effective-SNR to get the corresponding Symbol Error Rate (SER). The SER can be obtained by applying the Effective-SNR to the error performance estimation model for AWGN channel in (Fei Qin & John E Mitchell, 2011). The next step is to go through all four possible spreading code length modes, calculate the PER with the SER and packet length. It should be noted that different packet lengths will affect the error performance due to the CRC scheme. Finally, the spreading mode with maximized throughput will be returned as the optimized spreading code length mode.

As discussed in section 3.3, the Kalman filter implemented in our system will also track the change of environment noise in addition to the signal strength. Therefore, the Effective-SNR estimation will reflect the variation of both the signal strength and the environment noise. Obviously, the adaptation is not only optimized for the link quality but is also aware of changes in the environment noise, which will make the AS-MAC appropriate to be deployment in industrial locations with harsh RF environments where it will be able to track the change of environment noise strength, and deliver higher throughput when higher Effective-SNR exists in an opportunistic manner.

The optimization result will be embedded into an ACK packet and send back to the transmitter. The receiver will then be configured to the optimized spreading mode while waiting for the upcoming packet block. Since the ACK packet may also have the possibility of error, AS-MAC will start a timeout timer with the upper-limit of two packet intervals. In the case that the ACK packet is lost the timeout event will be triggered where the AS-MAC will stop the current receiving process and switch back to the idle state with the default spreading mode.

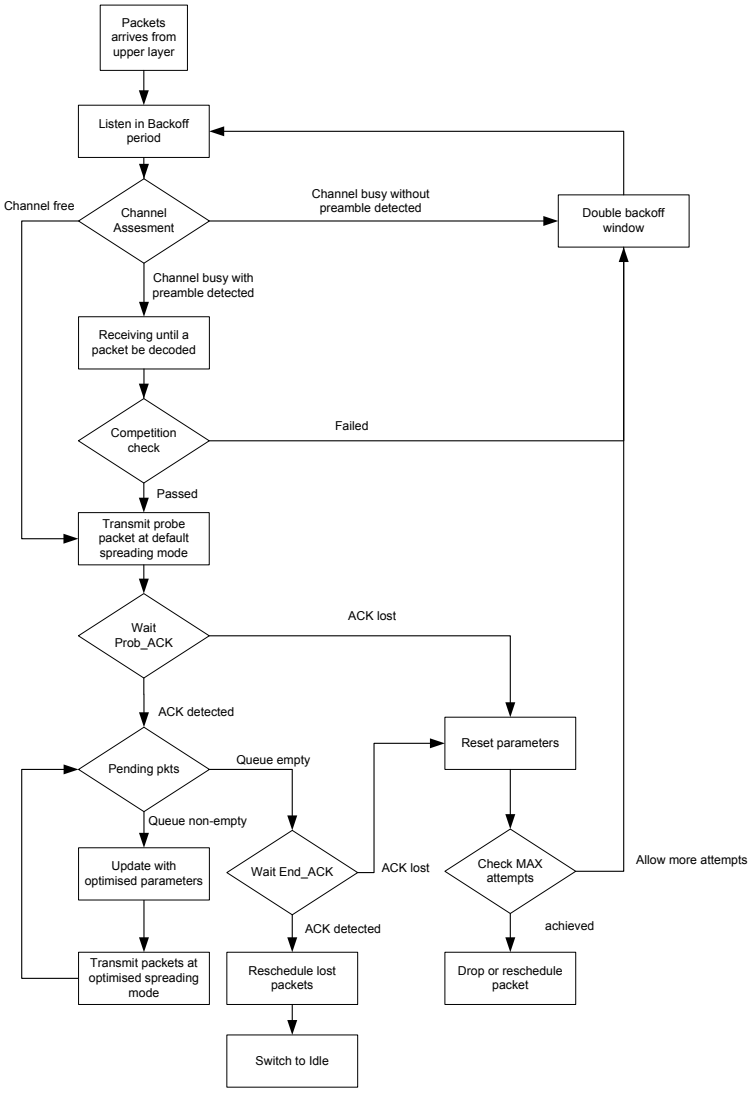

Fig. 7. Algorithm for transmission operation

3.5 Overall protocol architecture

Here, we will provide a description of the overall protocol architecture outlined by the algorithms in figure 8. The whole protocol will still be a random access based scheme but with modifications as discussed in previous sub-sections. When the MAC layer receives permission to send packets out, it will first enter the backoff state. Unlike the standard IEEE 802.15.4 the device will continue to assess the wireless channel during the backoff period to determine whether there are other activities on the channel. If the wireless channel is free (based on the current channel situation and history statistic), the protocol will transmit the first packet in the buffer queue[1] with the standard spreading modes and then wait for the ACK packet. This packet will be transmitted with either a single or dual use. When there are no other packets waiting in the queue, this operation will be exactly same a standard IEEE 802.15.4 MAC operation to deliver a single data packet. However, if there are more packets

[1] There should always be at least one packet in the queue, since the MAC layer will not be required to switch into transmission mode without a packet ready.

waiting in the queue, the first packet being transmitting will also have a second usage: as a probe packet (or RTS like IEEE 802.11 DCF). In this usage, the packet will not only deliver its own payload but will also carry a short field to notify the receiver that this operation will be a block transmission. The receiver, after successfully receiving the first packet as probe, will carry out an optimization process using the Kalman filter output to determine what is the best spreading mode for the current transmitter and embedded this information into the first ACK packet (perform the duty as a CTS packet if in IEEE 802.11 DCF). Then both the transmitter and receiver will switch to the optimized spreading modes to transmit the following packets with the channel-permitted highest datarate to increase the throughput while decrease the energy consumption. There will be a second ACK named as END_ACK after the block transmission, which will contain the ID of any lost packets. The transmitter will re-buffer the lost packets in that block into the queue and try to send them in another cycle as long as the queue is non-empty. If the END_ACK was lost, the system will follow the exponential backoff scheme, and start another cycle after the backoff period.

The system will be able to track and predict the change of link quality by employing a Kalman filter. In the case the Kalman filter has not converged, the system will work with the default, most robust spreading code length. As soon as the Kalman filter converges, the system carries out the optimization process and uses the optimized spreading code to deliver as high a throughput as possible, which will, of course, decrease the latency and reduce the energy consumption. It should also be noted that such a scheme should have almost the same energy efficiency with low offered traffic loads, but can trade the energy consumption for a better channel utilization with heavy offered traffic loads. We will experimentally demonstrate the system performances using this approach in the next section.

4. PERFORMANCE EVALUATION USING EXPERIMENTAL APPROACH

The proposed AS-MAC protocol has been implemented in a COTS platform (Dresden, 2009). This platform is equipped with 8MHz MCU, 128KB ROM space, and 10KB RAM space, which are comparable with most common WSNs platforms (e.g. MicaZ, TmoteSky). As a consequent, the proposed protocol implemented here should also be able to be implemented and work with almost all other WSN platforms. The standard IEEE 802.15.4 MAC protocol has been implemented as well to provide a direct comparison with the AS-MAC performance. The experiment location is an ordinary in-door environment, which suffers from multi-path effects due to reflections. Similarly to previous experiment in section 2, a vector signal generator, ESG4432B has been employed to generate the variable environment noise. The photo of experiment has been provided in figure 9.

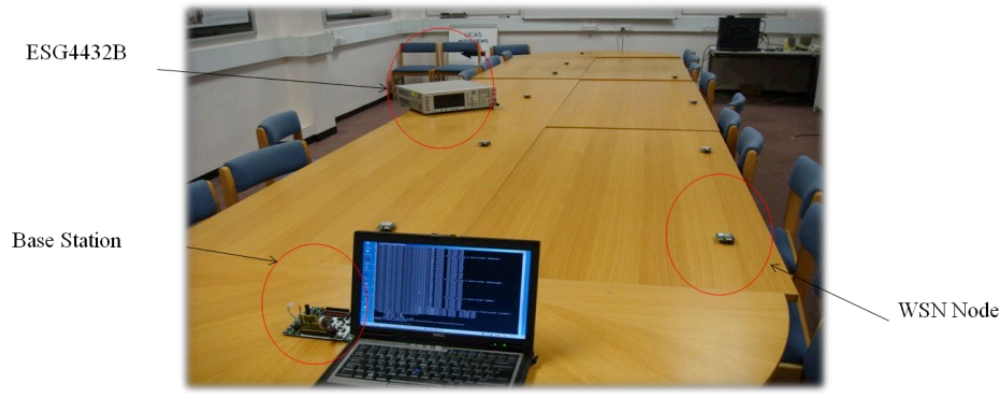

Fig. 8. General setup photo of the AS-MAC experiment

A series of experiments have been conducted to evaluate the proposed MAC protocol. The packet arrival rate was pre-configured before the experiment following a Poisson distribution with a mean value of □. Note that the default block contains 20 packets and the default payload length of a packet is 100 Bytes unless otherwise specified. In all the experiments the IEEE 802.15.4 MAC protocol and the AS-MAC have been configured with the default MAC parameters: the initial backoff window size W was set to 8, maximum retransmission attempts M was set to 4. To simplify the analyses, we disabled the retransmission scheme in both protocols, i.e. the protocol will drop the current packet in the event of ACK_Timeout being exceeded instead of re-adding it to the buffer queue for retransmission. As a result of this regulation, the offered traffic loads were determined only by the data arrival rate.

4.1 Throughput performance

We first explore the potential throughput capacity of the proposed AS-MAC by deploying only one transmission pair, where the channel collision probability can be eliminated. During the experiment, we increased the data arrival rate for the transmitter, i.e. increasing the offered traffic load in the system, until the system saturated. As expected, the standard IEEE 802.15.4 MAC is saturated at a packet arrival rate of 160 packets per second (pps), where the system is able to provide a total throughput (excluding MAC layer header and PHY layer preamble) of 118kbps. Therefore, the illustrated throughput in our work will be slight less than the offered traffic loads shown in figure 10, and may also be less than the reported value in other publications due to this calculation method. Then, as shown in figure 10, by enabling the adaptive spreading code length, the proposed AS-MAC allows increased throughput enabling the system to cope with an increasing offered traffic load of up to 260 pps. The maximum achieved throughput provided by AS-MAC could be as high as 204 kbps, which is a *76%* performance improvement comparing with the standard IEEE 802.15.4 MAC.

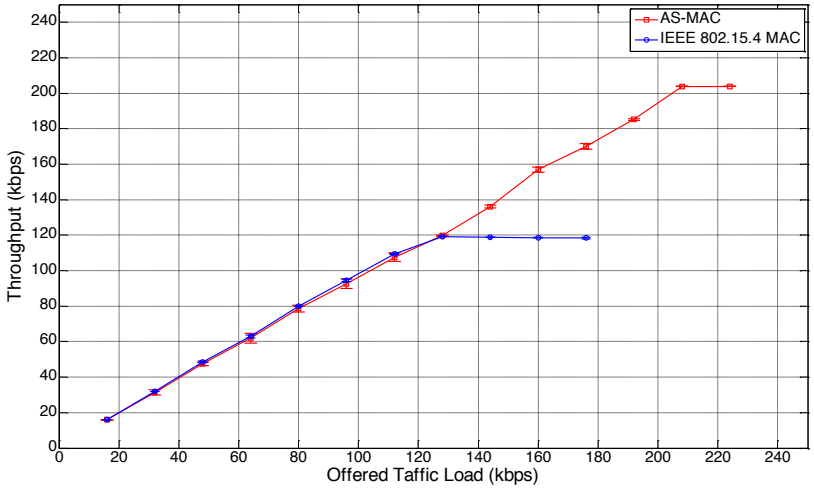

Fig. 9. Capacity comparison between the proposed AS-MAC and standard IEEE 802.15.4 MAC

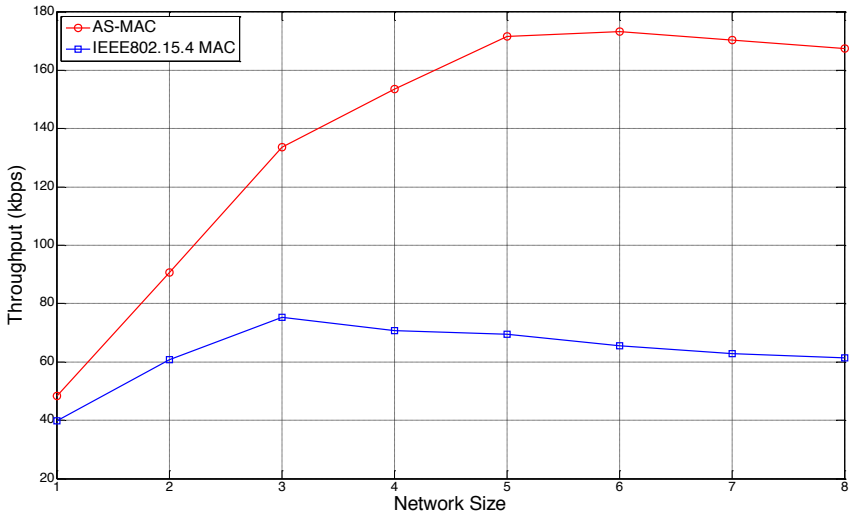

Fig. 10. Throughput performance in Star topology

The throughputs shown in figure 10 were monitored with a zero probability of collision in the wireless channel. As a result, the network throughput should be less than the maximum throughput shown in figure 10 when more nodes join the network and compete for the wireless channel. Therefore we deployed the protocol within a more realistic scenario to produce figure 11, where a certain number of nodes form a star topology based network. The packet arrival rate in each node has been configured to a fixed rate of 60 pps. Obviously, each newly joined node will increase the offered traffic load for the whole network and increase the collision probability. In the results shown in figure 11, the delivered throughput of the IEEE 802.15.4 MAC increased until the network exceeded 3 nodes and achieved a maximum throughput of 72.3 kbps. After this point, due to the increasing collision probability, the network throughput started to decrease with increasing network size. If we deployed the

proposed AS-MAC protocol within the same network scenario, as expected, the AS-MAC was able to support a higher offered traffic load, not peaking until the network reached 6 nodes. At this point, the AS-MAC delivered a throughput of 173.3 kbps which is a *139.7%* improvement over the standard IEEE802.15.4 MAC. Furthermore, if the results are compared with the capacity without collisions as shown in figure 10, it is seen that the standard IEEE 802.15.4 can only achieve *61.3%* of the capacity while AS-MAC is able to achieve higher ratio of *84.8%,* demonstrating the increase efficiency of the proposed AS-MAC.

The proposed protocol will still follow the general random access based MAC scheme, which means that the experiment throughput performance will be affected by the backoff settings as well. The results presented were captured with default backoff parameters (i.e. the initial backoff window size W was set to 8, maximum retransmission attempts M was set to 4). Nevertheless, if the experiment was configured with different parameters (e.g. a larger backoff window size), the peak point (i.e. the maximum achievable throughput, 3 in x axis for IEEE 802.15.4 and 6 for AS-MAC) will be moved to the right direction. This is because the device with a larger backoff window size will have a higher probability of successfully assessing the channel over other devices, which means the system will have better channel utilization ratio with a larger number of competing devices. At the same time, since a device will spent more time in the backoff period, the deliverable throughput will be decreased while the energy consumption may increase.

4.2 Throughput performance with exposed terminal and hidden terminal situation

In this section, we want to examine how the protocol might performance in multi-hop networks. It should be noted that two classic scenarios (exposed terminal and hidden terminal) are investigated here, which are typical in the multi-hop networks and are the main system performance limit in multi-hop scenarios. The performances of a true multi-hop scenario (i.e. 3 or 4 hops with 6 or 8 devices) are highly correlated with the location and route of devices. Hence, we consider the classic scenarios (hidden terminals and exposed terminals), as a baseline for multi-hop or mesh networks.

We first investigated the typical exposed terminal topologies consisting of two flows. In the topology shown in figure 12, node 1 and node 3 were transmitters and deployed within each other's transmission range. It should be noted that all devices in this experiment have been equipped with a 20dB attenuator to decrease the transmission range and simplify the experiment setup without any loss of accuracy. Therefore, through careful calibration node 0 has been deployed out of the effective range of node 3, i.e. node 0 cannot sense or receive any packet from 3. Following the same principle, node 2 has been deployed out of the effective range of node 1.

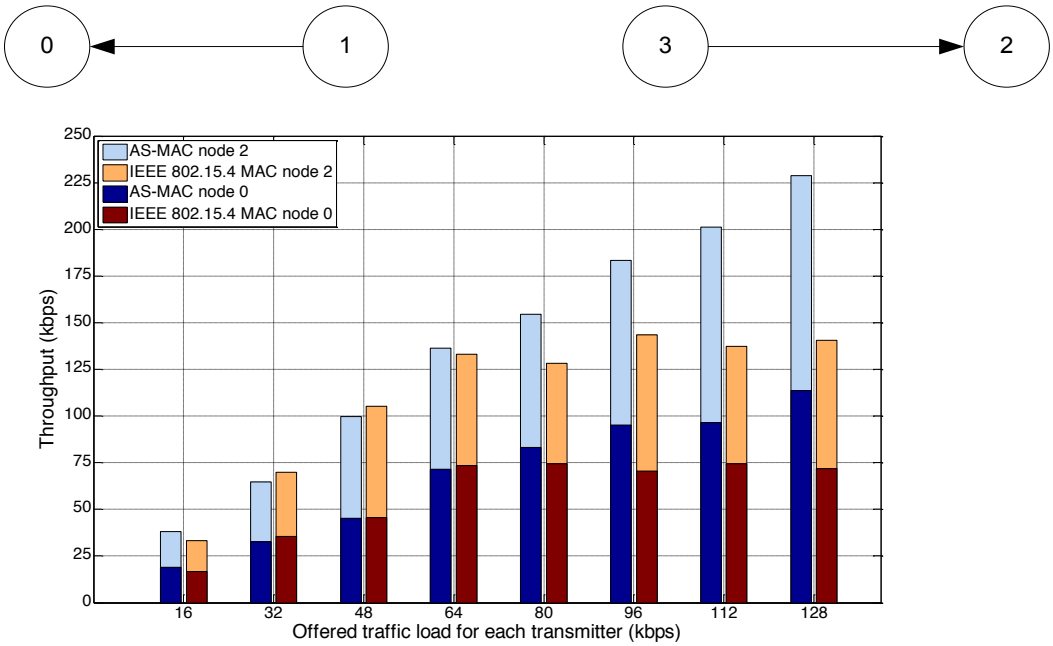

Fig. 11. Throughputs in exposed terminal scenario, node 1 and 3 are exposed terminals

As shown in figure 12, when the offered traffic load increases at both transmitters, the successfully delivered throughputs of flow 1->0 and flow 3->2 increase as well. However, due to the capacity of protocol, the IEEE802.15.4 MAC was saturated when the data arrival rate is 80 pps (64 kbps). After this point, the delivered throughput cannot maintain the offered traffic load and remains at a constant level. As a comparison, the AS-MAC can steadily increase until 160 pps (128 kbps), therefore increasing the total network throughput by *60.7%*. It should be noted that the total network throughput cannot go beyond the maximum throughput of a single flow in an ideal channel. However, in the experiment, the false channel sense assessment may enable the exposed terminals to transmit concurrently, slightly increasing the total system throughput delivered.

We now present an experiment with the topology shown in figure 13, which aims to evaluate the throughput performance in the hidden terminal scenario. Similarly to the topology shown in figure 12, both 1->0 and 3->2 flows have been deployed with sufficient link margin to achieve maximum throughput, while node 3 and 1 have been deployed out of the range of each other to replicate the hidden terminal scenario. In the standard IEEE 802.15.4 MAC, the carrier sensing scheme in node 1 may fail to detect the hidden terminal activity of node 3, and as a result the node 1 could access the channel, increasing the collision probability. Therefore, the delivered throughput in figure 13 shows an unfair pattern for the IEEE 802.15.4 MAC, i.e. the throughput of Node 0 has been limited to a relatively low value with respect to the total system throughput. As discussed in section 3, the introduction of a competition check in the AS-MAC is able to aid Node 3 in successfully avoiding the interruption of the transmission in link 1->0 by monitoring actions occurring in link 0->1. Therefore, as shown in figure 13, the system throughput can achieve an almost fair throughput performance among both flows, while the overall system throughput was also higher than standard IEEE 802.15.4 MAC because of the high datarate achieved by the shorter spreading code length modes.

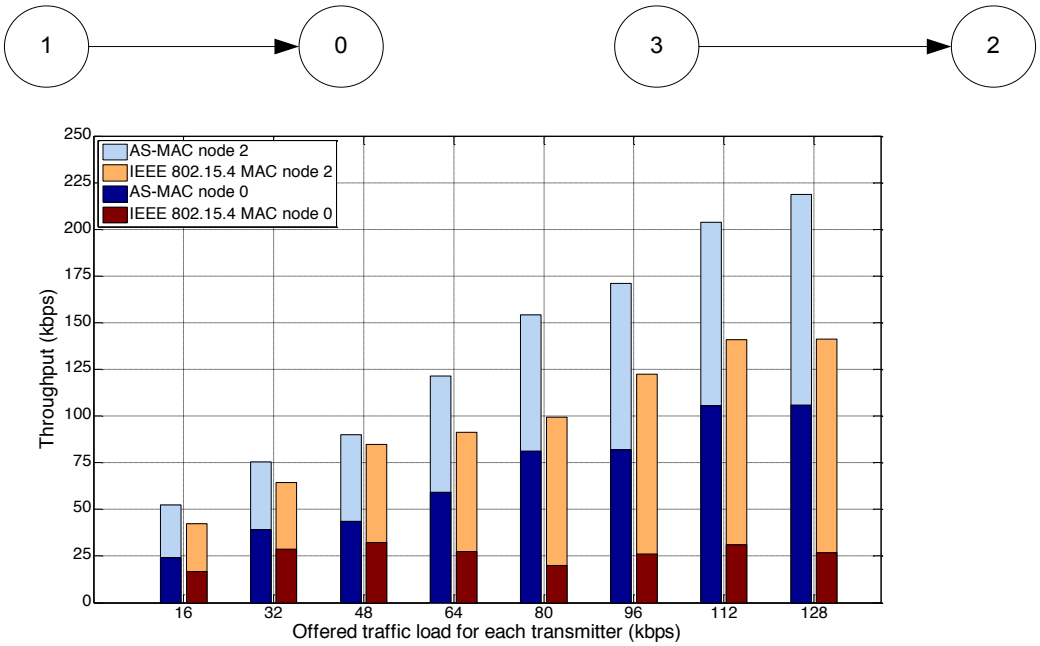

Fig. 12. Throughputs in hidden terminal scenario, node 3 is the hidden terminal of node 0

4.3 Throughput performance with variable environment noise

To evaluate the performance of the AS-MAC under the condition of channel noise, a vector signal generator ESG4432B has been employed to generate RF noise. The ESG4432B has been equipped with a 2.4GHz 0dBi antenna to feed noise directly into the wireless channel.

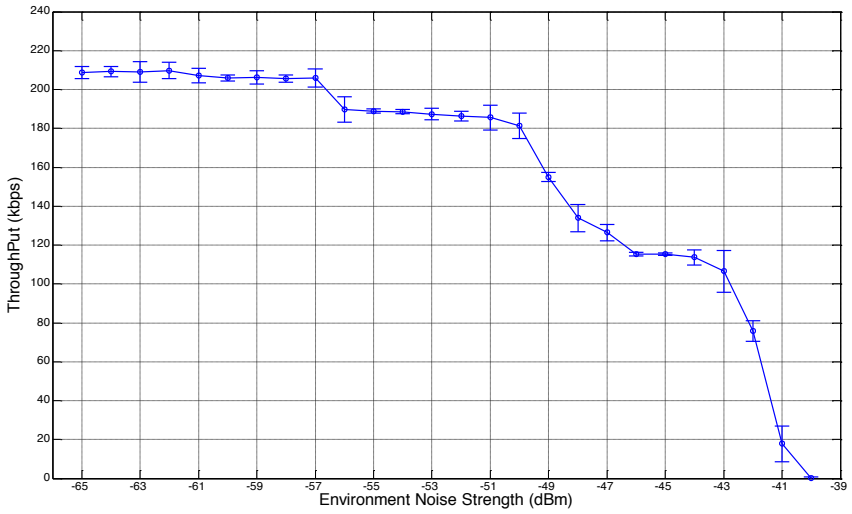

Fig. 13. Throughput performance with environment noise, single transmission pair

We first evaluated the performance of a single transmission flow with variable environment noise strengths. The transmitter has been configured with a fixed packet arrival rate 260 pps, which is almost the saturated state. The strength of environment noise is adjusted and the number of received packets at the receiver

side recorded to calculate the throughput. The results are provided in figure 14. The delivered throughput remains at its highest level of around 204 kbps until the environment noise exceeds -57dBm. It is assumed that before this point, the SNR was high enough for the transmission pair to work with the shortest spreading code length mode which can lead to the highest datarate. Consequently, when the environment noise was higher than -57dBm, the Kalman filter could learn this change in the environment and signal the AS-MAC to switch to the next spreading code length. This causes a reduction of the delivered throughput to around 185kbps. However, the third spreading mode was relatively hard to track in figure 14, since the SNR region for this mode is only 1dB (around -48dBm). Then, it is easy to notice that the algorithm will automatically switch to the lowest (i.e. the standard) spreading mode of IEEE802.15.4 around 118kbps from -46dBm to -43dBm. It should be noted that, in this situation the system will work in a similar mode to the block based transmission of WSNs (Hansen, 2010). In other words, if the system simply uses a block transmission based algorithm, then the maximum achievable throughput (in near saturated mode) or the capacity of a single transmission pair will be similar to the standard IEEE 802.15.4 system. This demonstrates that most of the performance improvement is due to spreading adaptation not block transmission. Beyond this point, although the system can still determine the decrease of the SNR margin, the system was fixed in this mode until the throughput trends to zero since there are no other modes for lower SNR margins. According to the motivation behind this protocol design, the experiment successfully demonstrates the ability of the protocol to be cognitive to the environment change and adjust itself to the best operating mode to maintain a reliable transmission link.

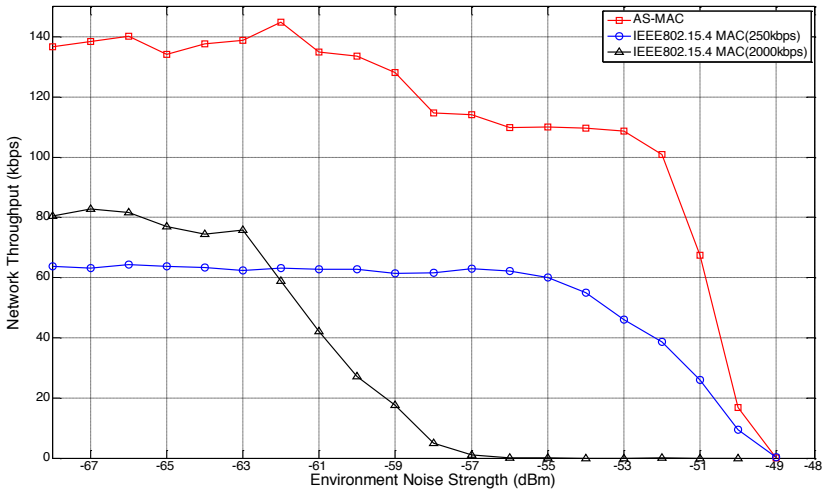

Fig. 14. Throughput performance with environment noise under star topology

We now evaluate the performance under environment noise in the more general star topology. The configuration of this experiment was almost the same as the previous experiment except the network consisted with three nodes with a packet arrival rate of 60 pps. Since there are three links in total, deployed in different locations, the link status will change in an uncorrelated fashion among nodes. Therefore, the combination of delivered throughputs shown in figure 15 is different to the result shown in figure 14. The overall deliverable throughput has been kept around 140kbps when the environment noise is lower than -62dBm. Then along with the increasing of environment noise to -58dBm, the delivered throughput decrease slowly to 110kbps. In the last stage, the throughput is going to decrease rapidly

toward zero, when the environment noise is higher than -53dBm. Generally, although the cognitive process of the AS-MAC is not as clear as the single device experiment, the system still shows the adaptively with the changing environment noise, while the standard IEEE 802.15.4 MAC has kept a relatively lower throughput around 60kbps just before reducing to zero. As a comparison, we also implemented another protocol which maintains the standard IEEE 802.15.4 MAC, except that the datarate has been forced to the highest rate. The result of this mode is shown as the black curve in figure 15. It demonstrates that without a carefully designed protocol, simply increasing the datarate cannot deliver consistently higher throughput due to the stability of the link.

Fig. 15. Experiment photo for protocol comparison with variable environment noise

The performance of the multi-flow scenario with environment noise was evaluated, as shown in figure 16. Devices configured for the AS-MAC and IEEE802.15.4 MAC have been deployed together, connected via a 2.4GHz Power Combiner/Divider to a single antenna to ensure that each pair of devices saw an identical wireless channel (with a 3dB degradation in transmit power due to the Combiner/Divider). The two nodes have been configured with the same ID but working in different RF channels. Consequently, the ESG4432B has been configured to generate an environment noise covering both channels.

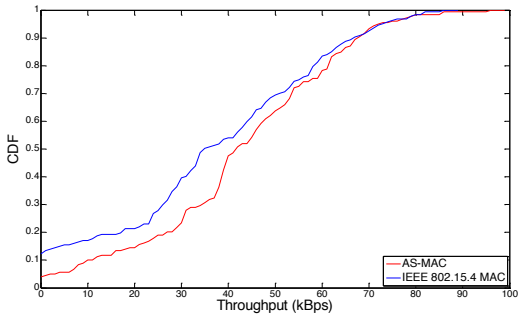

(a) packet arrival rate = 60 pps, spreading length = 32

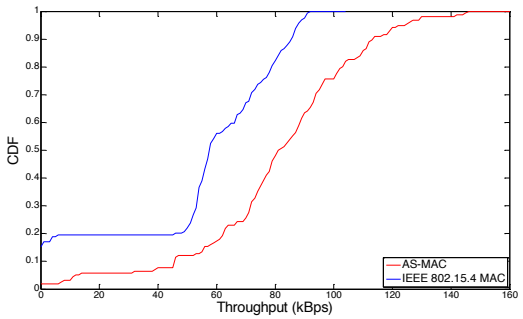

(b) packet arrival rate = 120 pps spreading length = 32

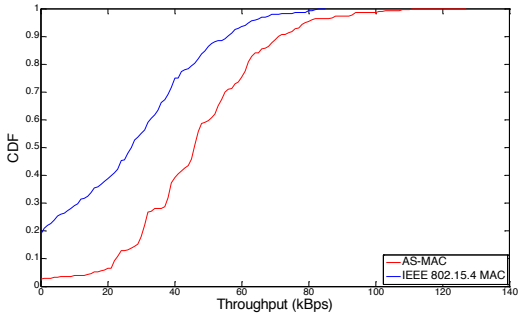

(c) packet arrival rate = 60 pps,, spreading length = 4

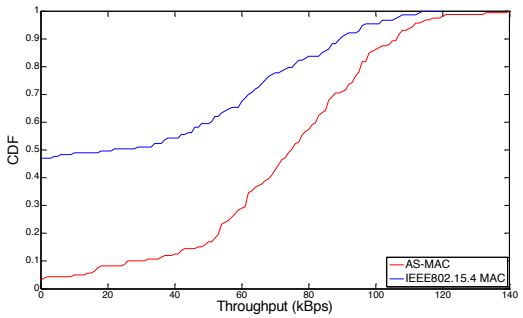

(d) packet arrival rate = 120 pps,, spreading length = 4

Fig. 16. Throughput performance with environment noise in the multi-flow scenario

A series of experiments have been implemented with this setup. Each of them was carried out with different MAC configurations, i.e. the offer traffic load and spreading code lengths. During each experiment, the strength of the environment noise was slowly adjusted from low to high and then reversed with the process being repeated several times. The receivers recorded and calculated the Cumulative Distribution Function (CDF) of the delivered throughput, which has been presented in figure 17. It should be noted that since these experiments involved manual manipulation of the experimental set-up (e.g. the physical process of connecting nodes to allow the uploading of new programmers may cause small movements of the devices location), we are unable to guarantee that the experiment conditions are exactly same for each of the four experiments. However, within each experiment the condition has been maintained for the two implemented protocols.

When the offered traffic load was low, i.e. 60 pps packet arrival rate, as the experiment result in figure 17 (a) shows, the delivered throughputs of AS-MAC and IEEE802.15.4 MAC show almost the same performance. However, when higher traffic loads occur, as high as 120 pps as shown in figure 17 (b), the AS-MAC can achieve higher throughput than the standard IEEE802.15.4 MAC. In the results

shown in figure 17 (c) and (d), we compared the AS-MAC with the standard IEEE 802.15.4 MAC with the shortest spreading code length. We see that this protocol can achieve higher throughput than the standard protocol but is still not able to deliver the throughput of the AS-MAC. This demonstrates that simply increasing the datarate could, in some circumstances expose the transmission link to a degraded link quality.

4.4 Energy efficiency

In this section, we will show the energy efficiency performance of the proposed AS-MAC. As discussed in previous sections, the AS-MAC should be able to achieve better energy efficiency by reducing the transmit time. To demonstrate this, a NI DAQ card (PCI 6209 with sample rate 10 kHz) has been employed to capture the current draw of the device during different operations. The integration of the recorded current allows us to derive the overall energy consumed by the device in that period, which is one of the most accurate ways to evaluate the energy efficiency of different MAC protocols.

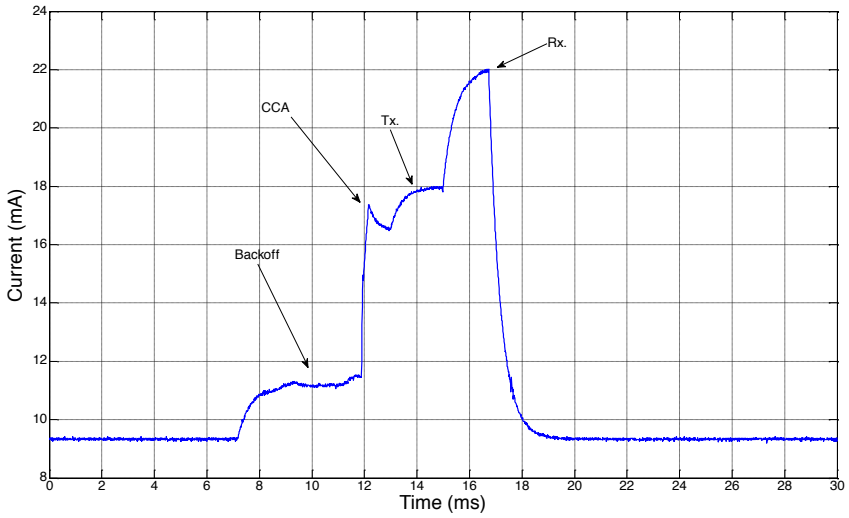

Fig. 17. Recorded power consumption of IEEE802.15.4 MAC

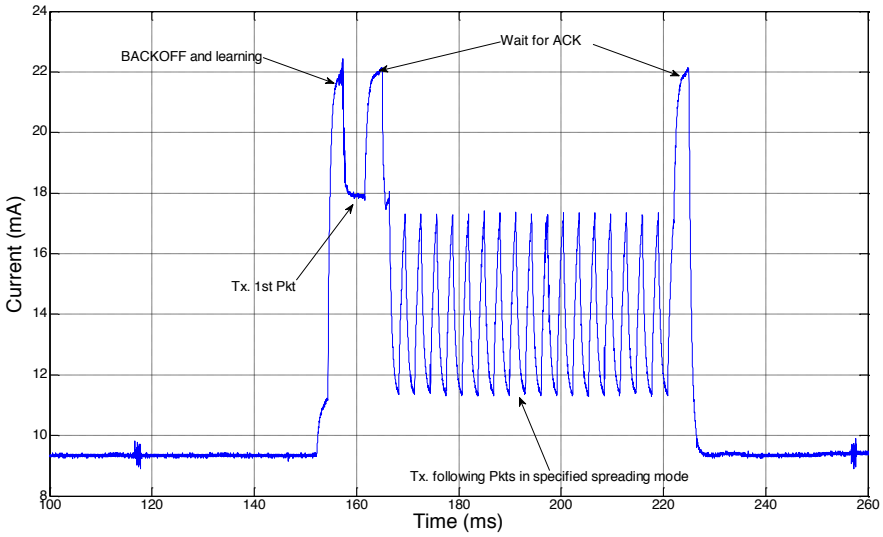

Fig. 18. Recorded power consumption of AS-MAC

Figure 18 and Figure 19 show the current consumption of IEEE 802.15.4 MAC and AS-MAC respectively. The devices we employed for experiment are equipped with capacitors to filter noise on the power lines which also leads to a low-pass filtering effect in the current monitoring system, i.e. a gradual transition between states. However, it should be noted that this effect will not degrade the accuracy of the analysis of energy efficiency. For the IEEE 802.15.4 MAC, we show the current drawn during the transmission of one packet: the device first enters the BACKOFF state for a random period, and then switch to the CCA state. If the CCA returns with a free channel event, the device will send the packet and then enter the RX state waiting for the ACK packet. Instead of one packet, we will show the power consumption of a block of packets for the AS-MAC which is more common in this protocol. As discussed in previous sections, the system also first enters the BACKOFF state, the difference is that the AS-MAC will enable receiving when in the BACKOFF state to gain as much as the channel information as possible, e.g. the exchange of packets. After the BACKOFF state, the MAC uses the information learned and historical data to decide whether the device can start the transmission. If it decides that it can, the device will send the first packet in the block as a probe packet. The receiver will then calculate the optimized spreading mode and reply with the ACK containing the optimization result. After receiving this ACK, the transmitter will send out the subsequent packets in the block with the optimized spreading code length. Then the transmitter will wait for the final ACK to report whether there have been any packets lost in this operation and arrange the retransmission if any.

Table I. Power Consumption for 1 hour in extremely low traffic load, Block_Size = 1 and packet arrival rate = 1 pps.

	IEEE802.15.4 MAC	AS-MAC
Power Consumption (mA Hour)	0.0197	0.0202

In section 1, we claimed that the AS-MAC should be compatible with traditional applications, i.e. the system offers extremely low traffic load (for example, 1 pps). Therefore, we evaluated the energy performance in this scenario, through the

configuration of Block_Size = 1 and packets arrival rate of 1 pps. The experiment lasted one hour for both protocols, and the two protocols show almost the same performance as seen in Table 1: AS-MAC consumed 0.0202 mAh, only slightly higher than the 0.0197 mAh of IEEE 802.15.4 MAC. If both systems were equipped with a standard 2000mAh battery, the system with IEEE 802.15.4 MAC can last 11.75 years, while the system with AS-MAC can last 11.45 years. The additional power is consumed by the increase in energy used in the BACKOFF state. However, due to the extremely low offered traffic load, the probability of channel contention has been limited as well. Therefore, the energy consumed by the BACKOFF state can be regulated to an affordable level as we discussed in section 1.

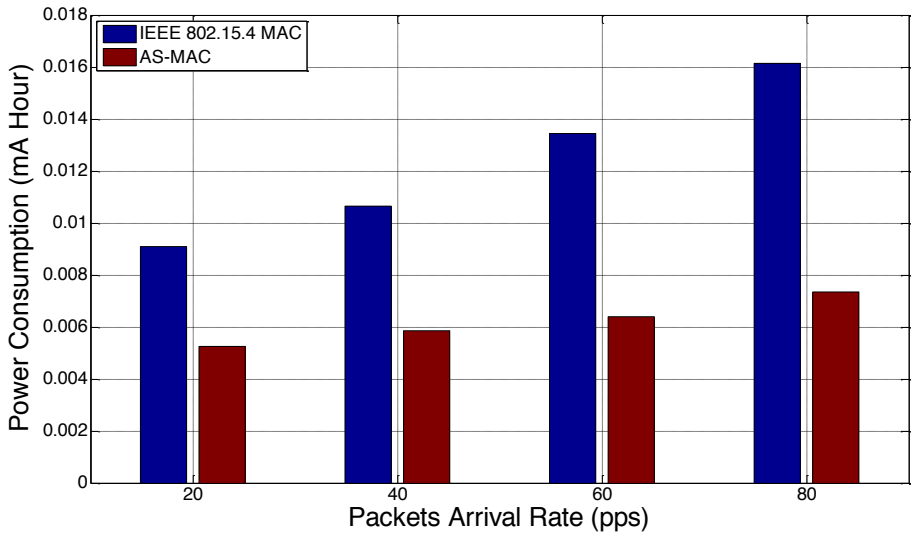

a) Power consumption with increased packets arrival rate for 10 min

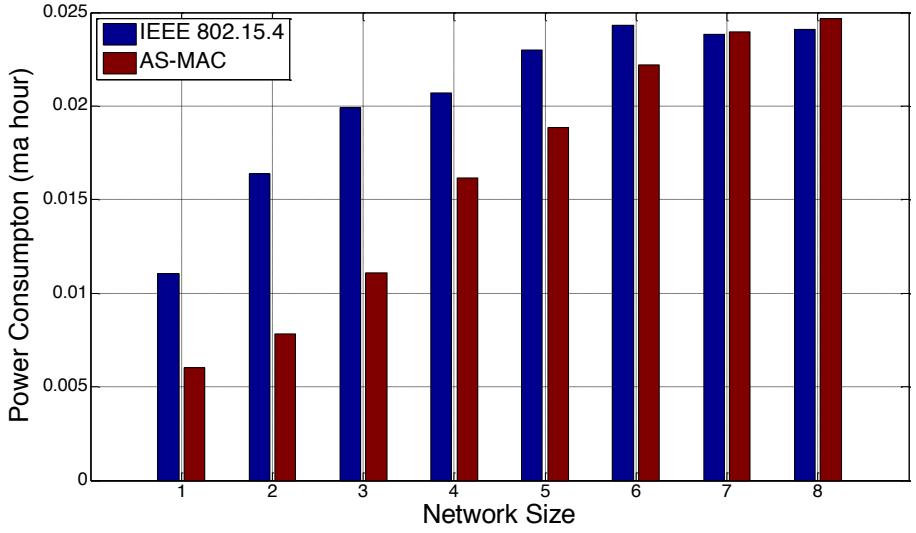

b) Power consumption with increased network size, 40 pps for 10 min

Fig. 19. Recorded power consumptions of device under various network configurations

Following the other experimental results analyzed in this section, we first evaluated the power consumption for a single transmission link. The offered traffic load has been increased from 20 pps to 80 pps, with each experiment lasting 10 minutes to record an average value of power consumption. As shown in figure 20.a, as the offered traffic load increases, the power consumption of the standard IEEE 802.15.4 MAC increases rapidly. As a comparison, the power consumption of AS-MAC increases much more slowly. For instance, when the packet arrival rate is 80 pps, the AS-MAC can save *54.3%* of the energy used by the IEEE 802.15.4 MAC.

We now evaluate the energy efficiency of the proposed AS-MAC in a general star topology. In the results shown in figure 20.b, both systems were offered a traffic load of 40 pps while the network size was constantly increasing. The system will consume more energy as the competition probability increases due to the scaling of the network size. In both systems, the energy consumption will increase until saturated (i.e. because of increased competition the device will have to be active all the time), the only difference is the speed at which this happens. It can be noticed that the energy consumption of IEEE 802.15.4 MAC will increase quickly at the beginning of experiment, i.e. with small competition, while the energy consumption of AS-MAC will increases faster during the later part, i.e. with heavy competition. If we recall the results in figure 10 and figure 11, we will find that in the similar network settings, the system will be saturated with overall offered traffic load of 160 pps (contributed by 4 devices with fixed traffic load) for IEEE 802.15.4 MAC, and with a network size of 6 (i.e.240pps or 6 devices) for AS-MAC. After that, because of the heavy offered traffic load, the competition probability also increases and therefore the AS-MAC consumes more energy in the BACKOFF state. In this situation, the AS-MAC can trade off this increase in energy usage for a better channel utilization which guarantees the delivered throughput in a high competition scenario.

As a conclusion, AS-MAC shows better energy efficiency than the IEEE 802.15.4 MAC in most situations. The increase traffic load itself will not increase the power consumption for AS-MAC (as figure20.a shows), but the increased competition probability coming with the increased traffic load will be more related with the energy efficiency of AS-MAC (as figure20.b shows). Even in heavy competition scenarios, the AS-MAC shows similar energy efficiency to the IEEE 802.15.4 MAC, while providing better deliverable throughput. We believe this is an overall profit to the network.

5. CONCLUSION

The design of this protocol has considered both the requirements of traditional WSN application and advanced WSN applications. Under low traffic load the system operation is very similar to the standard IEEE 802.15.4 system. However, once the system detected increased traffic load, the system can automatically enable the adaptive spreading code length mode to opportunistically utilize channel conditions to deliver packets as efficiently as possible. The proposed protocol jointly considers the signal strength, environment noise and competitors in the network to calculate the optimized spreading mode for the wireless sensor network. Our experimental results show that, in ordinary scenarios the AS-MAC can use less than half of the energy to deliver more than double of the throughput.

The advantages of proposed AS-MAC can be summarized as follows:

- The protocol will be able to deliver 139% higher throughput as well as having better energy performance than the standard IEEE 802.15.4 system.
- The protocol is robust to harsh RF environments by adapting the spreading code length to match the available link quality.
- The protocol is backwards compatible, e.g. it offers support for both extremely low duty cycle and data intensive scenarios.

- The implementation of the protocol is very low cost within resource constraint consideration.

Despite these benefits, the system based on the AS-MAC will also be able to provide multi-constraint QoS for the WSN systems which have different QoS requirements for different tasks running within one network. For instance, the MAC will report the current link capacity to the route layer, thus, the route protocol could assign links with high capacity to packets with higher priority. Since the link capacity will be adapted from time to time, the routing protocols will need to be able to self-learning. The investigation of compatible routing protocol will be a possible direction for future work.

REFERENCES

AGUAYO, D., BICKET, J., BISWAS, S., JUDD, G., & MORRIS, R. 2004. Link-level measurements from an 802.11 b mesh network. In Proceedings of the Conference on Applications, Technologies, Architectures, and Protocols for Computer Communications (SigComm04) . 121-132.

ANRITSU. (2011). Radio Frequency Interference in Hospitals.

ATMEL CO.LTD. (2009). AT86RF231 Datasheet.

CHEN, L. J., KAPOOR, R., SANADIDI, M. Y., & GERLA, M. 2004. Enhancing Bluetooth TCP throughput via link layer packet adaptation. In. Proceedings of IEEE International Conference on Communications (ICC).

DRESDEN. (2009). RCB128RFA1.

ESTEVES, E., BLACK, P. J., & GURELLI, M. I. 2002. Link adaptation techniques for high-speed packet data in third generation cellular systems. In Proceedings of European Wireless Conference (EW).

FEI QIN AND JOHN E MITCHELL 2011. Performance Estimation of Adaptive Spreading Code Length for Energy Efficient WSN. In. Proceedings of 7th IEEE Wireless Advanced Conference (WiAd).

FEI QIN, XUEWU DAI, AND JOHN E MITCHELL 2012. Estimate Effective-SNR for Wireless Sensor Network Using Kalman Filter. (Accepted by Ad Hoc Networks)

HANSEN, M. T. 2010. BTP: A Block Transfer Protocol for delay tolerant wireless sensor networks. In 35th IEEE Conference on Local Computer Networks (LCN) , 897-904.

HOLLAND, G., VAIDYA, N., & BAHL, P. 2001. A rate-adaptive MAC protocol for multi-hop wireless networks. In Proceedings of the 7th Annual International Conference on Mobile Computing and Networking (MobiCom) . 236-251.

IEEE STD.802.15.4. 2003. Wireless Medium Access Control (MAC) and Physical Layer (PHY) specifications for low-rate wireless personal area networks (LR-WPANs).

JOHNSTONE, I., NICHOLSON, J., SHEHZAD, B., & SLIPP, J. 2007. Experiences from a wireless sensor network deployment in a petroleum environment. In Proceedings of International Conference on Wireless Communications and Mobile Computing.

KALMAN, R. E. 1960. A new approach to linear filtering and prediction problems. Journal of basic Engineering, 82, 35-45.

KAMERMAN, A. & MONTEBAN, L. 1997. WaveLAN®-II: a high-performance wireless LAN for the unlicensed band. Bell Lab Technical Journal, 2, 118-133.

LANGENDOEN, K., BAGGIO, A., & VISSER, O. 2006. Murphy loves potatoes: Experiences from a pilot sensor network deployment in precision agriculture. In Proceeding of 20th IEEE International Parallel and Distributed Processing Symposium (IPDPS). 8.

LANZISERA, S., MEHTA, A. M., & PISTER, K. S. J. Reducing Average Power in Wireless Sensor Networks Through Data Rate Adaptation. In Proceedings of International Conference on Communication (ICC)..

O'ROURKE, D., FEDOR, S., BRENNAN, C., & COLLIER, M. 2007. Reception region characterisation using a 2.4 GHz direct sequence spread spectrum radio. In Proceedings of the 4th ACM Workshop on Embedded Networked sensors. ACM. 72.

RAHIMI, M., BAER, R., IROEZI, O. I., GARCIA, J. C., WARRIOR, J., ESTRIN, D. 2005. Cyclops: in situ image sensing and interpretation in wireless sensor networks. In Proceedings of the 3rd ACM International Conference on Embedded Networked Sensor Systems.. 204.

SEXTON, D., MAHONY, M., LAPINSKI, M., & WERB, J. 2005. Radio channel quality in industrial wireless sensor networks. In Proceedings of Sensor for Industry Conference. 88-94.

SHA, M., XING, G., ZHOU, G., LIU, S., & WANG, X. 2009. C-MAC: Model-driven concurrent medium access control for wireless sensor networks. In Proceedings of the 28th Annual IEEE International Conference on Computer Communications (INFOCOM). IEEE.

SUKUN, K., PAKZAD, S., CULLER, D., DEMMEL, J., FENVES, G., GLASER, S. et al. 2007. Health Monitoring of Civil Infrastructures Using Wireless Sensor Networks. In Proceedings of Information Processing in Sensor Networks (IPSN). 254-263.

TANG, L., WANG, K. C., HUANG, Y., & GU, F. 2007. Channel characterization and link quality assessment of IEEE 802.15. 4-compliant radio for factory environments. IEEE Transactions on Industrial Informatics, 3, 99-110.

VUTUKURU, M., BALAKRISHNAN, H., & JAMIESON, K. 2009. Cross-layer wireless bit rate adaptation. ACM SIGCOMM Computer Communication Review, 39, 3-14.

VUTUKURU, M., JAMIESON, K., & BALAKRISHNAN, H. 2008. Harnessing exposed terminals in wireless networks. In Proceedings of the 5th USENIX Symposium on Networked Systems Design and Implementation 59-72.

ZHANG, J., TAN, K., ZHAO, J., WU, H., & ZHANG, Y. 2008.A practical SNR-guided rate adaptation. In Proceedings of the 27th Annual IEEE International Conference on Computer Communications (INFOCOM).. 2083-2091.

Received Jan. 2012; revised Oct. 2012; accepted XX 2012